Electron acceleration from rest in vacuum by an axicon Gaussian laser beam

Yousef I. Salamin*
Physics Department, American University of Sharjah, P.O. Box 26666, Sharjah, United Arab Emirates
(Received 14 November 2005; published 7 April 2006)

We employ the lowest-order radially polarized axicon fields of a Gaussian laser beam to demonstrate that electrons may be accelerated from rest in vacuum to a few GeV. Petawatt power laser beams focused onto micron-size focal spots result in multi-TeV/m electron energy gradients.

DOI: 10.1103/PhysRevA.73.043402 PACS number(s): 42.50.Vk, 42.65.−k, 52.75.Di

I. INTRODUCTION

For electrons to be accelerated and reach a net maximum energy gain from interaction with the fields of a laser beam, in any of the schemes discussed thus far, the beam must be focused onto small spatial dimensions [1]. Focusing, in turn, causes all mutually perpendicular $\boldsymbol{E}$ and $\boldsymbol{B}$ field components to appear in the focal region [2–8]. Besides the $\boldsymbol{v}\times\boldsymbol{B}$ force, the forward electric field component—say, E_z—plays a dominant role in accelerating the electron [9,10]. This has been demonstrated in theoretical simulations [1,5–8,11–20] as well as in experiments, in vacuum [21], and in plasma-based [22–25] schemes. Linearly polarized laser beams have predominantly been used in these investigations.

More promising configurations for electron-laser acceleration could be ones that employ radially polarized beams. Since one way to generate radially polarized light [26,27] involves using axicon optical elements, the associated fields will often be referred to here as *axicon fields* [28]. The lowest-order axicon fields [11,28,29] possess nonzero radial and axial electric field components E_r and E_z, respectively, in addition to an azimuthal magnetic field component B_θ. In a setup to accelerate electrons, the axial electric field component serves the purpose of acceleration directly quite well, while the remaining field components help to trap the electrons and may result in a high-quality accelerated electron beam [29,30].

Recent experiments [31,32] have demonstrated that a radially polarized laser beam may be focused onto a spot significantly smaller than would be the case for a linearly polarized beam. Under the conditions of their experiment, Dorn and co-workers [32] have shown that as much as 72.8% of the total beam power could be concentrated in the longitudinal field. In this paper, we demonstrate that an electron may gain as much as 3 GeV from interaction with that power derived from a highly intense ($\sim 10^{22}$ W/cm^2) beam, focused down to a waist radius of ~ 1 μm. This will be done by numerically solving the equations of motion of a single electron in the lowest-order fields of the radially polarized laser beam.

The axicon modes of a Gaussian beam will be employed. In their description, the well-known parameters of a Gaussian beam will be utilized. Single-electron calculations will be made assuming the electron is born at rest (perhaps from some ionization process) at the origin of a Cartesian coordinate system. The origin will serve as a stationary focus and the z axis as the direction of propagation.

In an attempt at making this paper independently readable the axicon fields will be derived and briefly discussed in Sec. II. The discussion involves the power and intensity relationships of relevance to the subsequent calculations. In Sec. III the equations of motion of a single electron in the axicon fields will be given and the method of their numerical solution leading to the energy gain and actual trajectories, among other dynamical aspects, will be outlined. This will be followed by Sec. IV presenting and discussing electron acceleration and the roles played in the process by various laser parameters and initial conditions. Our conclusions will be given in Sec. V.

II. THE FIELDS

Derivation of the lowest-order axicon Gaussian fields will follow the work of McDonald [28], almost step by step, apart from a slight change of notation, the use of SI units throughout, and the assumption that the fields (of wavelength λ) have a time dependence of the form $e^{i\omega t}$, where ω is the frequency. This is done here merely in order to make the paper self-contained. Recall that, in addition to the frequency ω, two parameters determine the fields of a Gaussian beam: namely, its waist radius at focus, w_0, and its Rayleigh range $z_r=\pi w_0^2/\lambda$ (and, hence, the diffraction angle $\varepsilon\equiv w_0/z_r$) [1–4]. The same parameters will be employed in describing the axicon fields, hence the designation *axicon Gaussian*. Propagation along the z axis and a stationary focus at the origin O will be assumed. According to McDonald [28], the axicon modes of a Gaussian laser beam, having a wave number $k=\omega/c$, with c the speed of light in vacuum, may be derived from a longitudinally polarized vector potential $\boldsymbol{A}$ and the corresponding scalar potential Φ. To begin with, the vector potential satisfies the wave equation

$$\nabla^2\boldsymbol{A}=\frac{1}{c^2}\frac{\partial^2\boldsymbol{A}}{\partial t^2} \tag{1}$$

and is related to the scalar potential Φ by the Lorenz condition (SI units will be used throughout)

*Electronic address: ysalamin@aus.edu

$$\nabla \cdot \boldsymbol{A} + \frac{1}{c^2}\frac{\partial \Phi}{\partial t} = 0. \tag{2}$$

The electric and magnetic fields then follow from the potentials, as usual, by differentiation:

$$\boldsymbol{E} = -\nabla\Phi - \frac{\partial \boldsymbol{A}}{\partial t}, \quad \boldsymbol{B} = \nabla \times \boldsymbol{A}. \tag{3}$$

Employing cylindrical coordinates (r,θ,z), where the z axis is aligned with the laser beam propagation direction, the desired fields may be obtained from

$$\boldsymbol{A}(r,\theta,z,t) = \hat{z}\Psi(r,z)g(\eta)e^{i\eta}. \tag{4}$$

Here $g(\eta)$ is a pulse-shape function depending upon the plane-wave phase $\eta=\omega t-kz$ and $\hat{z}$ is a unit vector along the positive z axis. With the assumed time dependence of the fields, direct substitution of this trial solution into the wave equation yields

$$\nabla^2\Psi - 2ik\frac{\partial \Psi}{\partial z}\left(1 - i\frac{g'}{g}\right) = 0, \tag{5}$$

where $g' \equiv dg/d\eta$. For a pulsed laser beam, one must have $g' \ll g$, a condition we will use repeatedly in our derivations leading to the fields [28]. Eventually, since we are interested in the fields of a continuous beam, we will set $g=1$. When the term g'/g is dropped from Eq. (5) and after the scaled coordinates

$$\rho = \frac{r}{w_0}, \quad \zeta = \frac{z}{z_r} \tag{6}$$

have been employed in it, it transforms into

$$\nabla_\perp^2\Psi - 4i\frac{\partial \Psi}{\partial \zeta} + \varepsilon^2\frac{\partial^2\Psi}{\partial \zeta^2} = 0, \quad \nabla_\perp^2 \equiv \frac{1}{\rho}\frac{\partial}{\partial \rho}\left(\rho\frac{\partial}{\partial \rho}\right), \tag{7}$$

with the diffraction angle defined by $\varepsilon = w_0/z_r$. Note that ε^2 is a small quantity and may thus be used as an expansion parameter for Ψ. So, let us write

$$\Psi = \Psi_0 + \varepsilon^2\Psi_2 + \varepsilon^4\Psi_4 + \cdots. \tag{8}$$

Next this is inserted into Eq. (7). When terms of order ε^n, where $n=0,2,4,\ldots$, are collected, there results

$$\nabla_\perp^2\Psi_0 - 4i\frac{\partial \Psi_0}{\partial \zeta} = 0, \tag{9}$$

$$\nabla_\perp^2\Psi_2 - 4i\frac{\partial \Psi_2}{\partial \zeta} + \frac{\partial^2\Psi_0}{\partial \zeta^2} = 0, \tag{10}$$

$$\nabla_\perp^2\Psi_4 - 4i\frac{\partial \Psi_4}{\partial \zeta} + \frac{\partial^2\Psi_2}{\partial \zeta^2} = 0, \tag{11}$$

$$\vdots$$

For our purposes in this paper, only the lowest-order fields will be sought. Those may be obtained from the paraxial approximation, Eq. (9). The well-known paraxial solution is

$$\Psi_0 = fe^{-f\rho^2}, \quad \text{with } f = \frac{i}{\zeta + i} = \frac{e^{i\tan^{-1}\zeta}}{\sqrt{1+\zeta^2}}. \tag{12}$$

Thus, in the paraxial approximation, the vector potential will be given by (setting $g=1$)

$$\boldsymbol{A} = \hat{z}A_0 fe^{-f\rho^2}e^{i\eta}, \quad A_0 = \text{const}. \tag{13}$$

Next we employ an ansatz for the scalar potential similar to that of the vector potential: namely, $\Phi = g(\eta)\phi(r,\theta,z)e^{i\eta}$. This gives $\partial\Phi/\partial t = i\omega\Phi(1 - ig'/g) \approx i\omega\Phi$. Hence, the Lorenz condition yields

$$\Phi = \frac{ic}{k}\nabla \cdot \boldsymbol{A}. \tag{14}$$

Finally, Eqs. (3) give, for the electric and magnetic fields,

$$\boldsymbol{E} = -i\omega\boldsymbol{A} - \frac{ic}{k}\nabla(\nabla \cdot \boldsymbol{A}), \quad \boldsymbol{B} = \nabla \times \boldsymbol{A}. \tag{15}$$

The following, hitherto *complex*, lowest-order electric field components follow from some tedious algebra which we omit here in order to save space:

$$E_r = E_0\varepsilon\rho f^2 e^{-f\rho^2}e^{i\eta} + O(\varepsilon^3), \quad E_0 = \omega A_0, \tag{16}$$

$$E_\theta = 0, \tag{17}$$

$$E_z = -iE_0\varepsilon^2(1 - f\rho^2)f^2e^{-f\rho^2}e^{i\eta} + O(\varepsilon^4). \tag{18}$$

Likewise, the *complex* magnetic field components turn out to be $B_r=0, B_\theta = E_r/c$, and $B_z=0$. Finally, the *real* axicon fields may be written down from Eqs. (16)–(18) as

$$E_r = \varepsilon E_0\left(\frac{w_0}{w}\right)^2\left(\frac{r}{w_0}\right)e^{-r^2/w^2}\cos\psi, \quad E_\theta = 0, \tag{19}$$

$$E_z = \varepsilon^2 E_0\left(\frac{w_0}{w}\right)^2 e^{-r^2/w^2} \times\left[\left(1 - \frac{r^2}{w^2}\right)\sin\psi - \left(\frac{z}{z_r}\right)\left(\frac{r}{w}\right)^2\cos\psi\right], \tag{20}$$

$$B_r = 0, \quad B_\theta = \frac{E_r}{c}, \quad B_z = 0. \tag{21}$$

In Eqs. (19) and (20), $w = w_0\sqrt{1+(z/z_r)^2}$ and the trigonometric functions have the same argument

$$\psi = \psi_0 + \omega t - kz - \left(\frac{z}{z_r}\right)\left(\frac{r}{w}\right)^2 + 2\tan^{-1}\zeta, \tag{22}$$

where ψ_0 is a constant (initial) phase. Note that E_r vanishes at all points on the z axis, $r=0$. Thus, charged particles initially injected axially do not feel the effect of the radial electric field component and continue to move, without deflection, along the z axis. On the other hand, the radial field component peaks at $r = w_0/\sqrt{2}$, with a peak value there given by

$$E_{r0} = \frac{\varepsilon E_0}{\sqrt{2e}}, \quad e \approx 2.7183. \tag{23}$$

Furthermore, E_z is most pronounced for points on the z axis where it is needed for particle acceleration. As a matter of fact, the axial electric field attains a maximum

$$E_{z0} = \varepsilon^2 E_0, \tag{24}$$

right at the beam focus, $r=0=z$. Thus an electron, for example, born at rest at the origin of coordinates would be immediately subjected to the maximum axial electric field component and may, thus, be maximally accelerated provided action of the field on it commences at the right moment (when the field has the right initial phase ψ_0). Note further that

$$E_{z0} = \varepsilon\sqrt{2e}E_{r0} \cong 0.7422\left(\frac{\lambda}{w_0}\right)E_{r0}. \tag{25}$$

For the purpose of electron acceleration it is desirable to make the axial field as large as possible. According to Eq. (25) it would be possible for the maximum axial field amplitude to exceed that of the radial field, provided the laser beam may be focused to a waist radius w_0 less than 0.7422λ.

Now with $\boldsymbol{E}=\hat{\boldsymbol{r}}E_r+\hat{\boldsymbol{z}}E_z$ and $\boldsymbol{B}=\hat{\boldsymbol{\theta}}B_\theta$, where $\hat{\boldsymbol{r}}$ and $\hat{\boldsymbol{\theta}}$ are unit vectors in the directions of increasing cylindrical coordinates r and θ, respectively, the Poynting vector takes the form

$$\boldsymbol{S} = \frac{1}{c\mu_0}(\hat{\boldsymbol{z}}E_r^2 - \hat{\boldsymbol{r}}E_rE_z), \tag{26}$$

with μ_0 the permeability of free space. An expression for the total power of the laser system may be obtained by integrating the z component of the Poynting vector over the beam cross section through its focus and then taking the time average of the result. This process gives

$$P \equiv \int_0^\infty \langle \boldsymbol{S}\cdot\hat{\boldsymbol{z}}\rangle 2\pi r dr = \left(\frac{\lambda^2}{8\pi c\mu_0}\right)E_0^2, \tag{27}$$

where $\langle\cdots\rangle$ stands for time averaging. In terms of P, the peak intensity may be written as

$$I_0 \equiv \langle \boldsymbol{S}\cdot\hat{\boldsymbol{z}}\rangle_{r=w_0/\sqrt{2},z=0} = \frac{2P}{\pi e w_0^2}. \tag{28}$$

This gives a peak intensity

$$I_0\ [\mathrm{W/cm^2}] \simeq 2.342\times 10^{22}\ P\ [\mathrm{PW}]/(w_0\ [\mu\mathrm{m}])^2. \tag{29}$$

According to Eq. (29), a petawatt ($P=1$) laser beam focused onto $w_0=1$ μm waist radius has a peak intensity of $I_0 \simeq 2.342\times 10^{22}$ W/cm^2.

It is interesting to compare the relative strength of the electric field components. In Figs. 1(a) and 1(b) we show $\langle|E_r/E_{r0}|^2\rangle$ and $\langle|E_z/E_{r0}|^2\rangle$, respectively, as functions of r/w_0 in the transverse plane ($z=0$) through the origin of coordinates. As expected, the peak in (a) occurs at $r/w_0=1/\sqrt{2}$, and in (b) the main peak occurs at $r/w_0=0$ in addition to a much less pronounced peak at $r/w_0=\sqrt{2}$, as may easily be shown analytically. It should also be clear that the secondary peak in (b) occurs due to an axial field whose direction is the opposite of that corresponding to the main peak. In between the two peaks an intensity minimum of zero occurs (at $r/w_0=1$), which corresponds to the point at which the field changes direction between oscillations. In Fig. 1(c), $\langle|E_z/E_{z0}|^2\rangle$ is shown along the propagation direction ($r=0$) as a function of z/z_r. Notice that the axial field amplitude, scaled by E_{r0}, is proportional to $\varepsilon=2/kw_0$ and, hence, the axial field intensity in Fig. 1(b) is inversely proportional to w_0^2. By contrast, the radial and axial field intensities shown in Figs. 1(a) and 1(c) are independent of w_0.

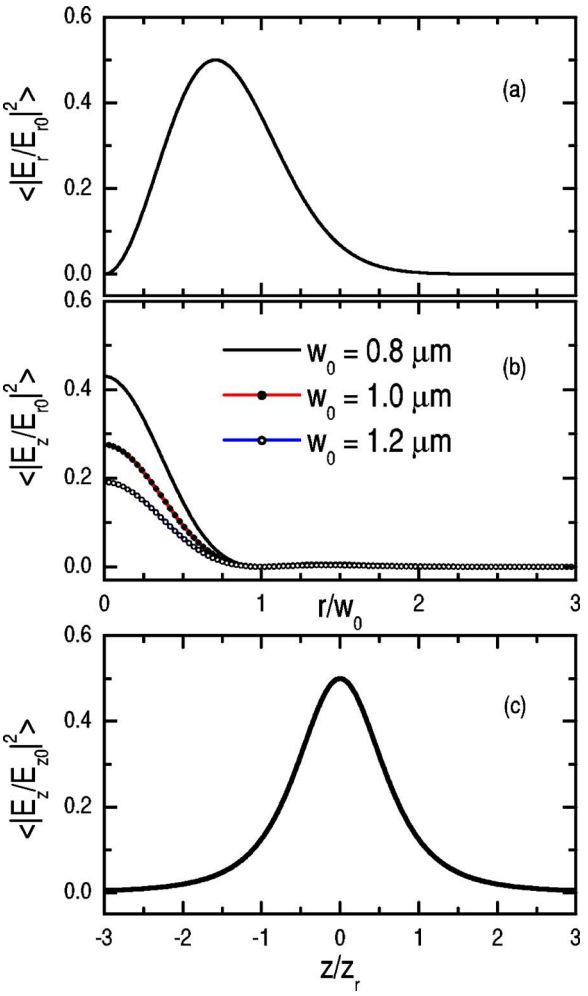

FIG. 1. (Color online) (a) The radial field intensity and (b) the axial field intensity in the transverse plane through the focus as functions of the radial distance r in units of w_0. (c) The axial field intensity along the propagation direction.

III. DYNAMICS AND ENERGY GAIN CALCULATIONS

Only single-electron dynamics in the fields of Sec. II will be pursued in the remainder of this paper, and for that purpose we resort to the fully relativistic equations of motion of a single electron (of mass m and charge $-e$) in the axicon fields of Eqs. (19)–(21). The equations of motion read

$$\frac{d\boldsymbol{p}}{dt} = -e[\boldsymbol{E} + c\boldsymbol{\beta} \times \boldsymbol{B}], \quad \frac{d\mathcal{E}}{dt} = -ec\boldsymbol{\beta} \cdot \boldsymbol{E}, \tag{30}$$

where the electron's momentum and total energy are given by $\boldsymbol{p} = \gamma mc\boldsymbol{\beta}$ and $\mathcal{E} = \gamma mc^2$, respectively. In these expressions, $\gamma = (1-\beta^2)^{-1/2}$ is the Lorentz factor of the electron. Unfortunately, analytic work based on Eqs. (30) is hard to come by, apart from very specialized situations involving plane-wave fields. For tightly focused fields, however, numerical integration of these equations is inevitable. Equations (30) may be coupled into a single equation for the scaled velocity: namely,

$$\frac{d\boldsymbol{\beta}}{dt} = \frac{e}{\gamma mc}[\boldsymbol{\beta}(\boldsymbol{\beta} \cdot \boldsymbol{E}) - (\boldsymbol{E} + c\boldsymbol{\beta} \times \boldsymbol{B})], \tag{31}$$

whose three scalar components may then easily qualify for simultaneous solution using a Runge-Kutta routine. In general, the initial conditions (holding at $t=0$) involve an injection-scaled velocity $\boldsymbol{\beta}_0$ and an injection point in space (x_0, y_0, z_0). The value of β_0 follows from the injection energy $\gamma_0 mc^2$, with $\gamma_0 = (1-\beta_0^2)^{-1/2}$. In a typical calculation, integration of the equations of motion will be carried out over the time interval $(0, NT)$, where $T = \lambda/c$ is one laser field period and N is a large integer. To ensure stability of the integrations, $\eta = \omega t - kz$ will be used as an integration variable instead of the time t. In all our calculations, we take $\eta_{max} = 4\pi$, which corresponds to $N = 2 + z_{max}/\lambda$, where z_{max} is the maximum forward excursion of the electron. Typically, N is of the order of $10^7 - 10^8$. From the integration one gets the scaled velocity $\boldsymbol{\beta}$ and, hence, the Lorentz factor γ of the ejected electron. Finally, one calculates the energy gain from

$$(\text{Gain}) = (\gamma - \gamma_0)mc^2. \tag{32}$$

Other dynamical aspects of the electron motion may be calculated as well. Further numerical integrations give the electron trajectory equations in terms of the time as a parameter, from injection to ejection. One may also monitor the momentum components of the electron and components of the force acting on it along its trajectory, which can shed valuable light on the mechanism of acceleration.

IV. ACCELERATION FROM REST

We consider now the important special case of acceleration of an electron born at rest, perhaps from ionization of an atom, at the center of coordinates. For such a case, the initial conditions are $\boldsymbol{\beta}_0 = 0$ and $x_0 = y_0 = z_0 = 0$. The vanishing of E_r on axis leaves E_z to accelerate the electron axially. Note that B_θ acts also to confine the electron and keep it on the z axis. Our numerical calculations confirm that the electron trajectory is straight along z, as may also be verified by inspection of the first of Eqs. (30).

The (initial) phase constant ψ_0 plays a crucial role, as always, in determining the subsequent electron motion and associated energy gain. Simply put, if the electron initially (at $t=0$) encounters a positive (forward) axial electric field component, the force on it would be repulsive and it would start moving backwards. So in order to reach a maximum energy gain, the laser-electron interaction should commence at some optimal initial phase value, which we seek first. To that end, we calculate the gain corresponding to the entire range of ψ_0 from 0 to 2π. The results are displayed in Fig. 2.

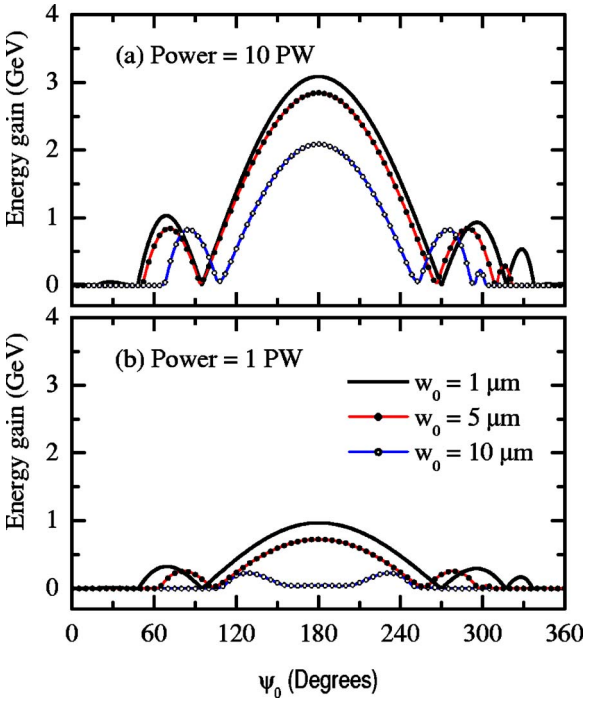

FIG. 2. (Color online) Electron energy gain as a function of the (initial) constant phase ψ_0. Parameters not shown include: wavelength $\lambda = 1$ μm, $x_0 = y_0 = z_0 = 0$, $\gamma_0 = 1$, and integration is over $10^7 - 10^8$ field cycles. Note that the legends in (b) apply to (a) as well.

Conclusions drawn from Fig. 2 include the following. First, the gain peaks for $\psi_0 \simeq \pi$ which corresponds to synchronized *injection* and, therefore, minimum slippage. To see this clearly, note that the (accelerating) axial field component E_z is zero at the origin (for $\psi_0 = \pi$) and is negative (and increasing in magnitude) during a full half cycle. Riding with the field (synchronization) during that half cycle, the electron gains maximum energy compared to situations in which $\psi_0 \neq \pi$. Second, in those cases, the maximum gain exceeds 3 GeV, compared to the maximum of about 2 GeV obtained in similar calculations when typically MeV electrons are injected into the focal region of a linearly polarized Gaussian beam [1,5–8]. Our results also agree with the (plane-wave) estimate of a maximum interaction energy equal to $mc^2q^2/4$, where q^2 is a dimensionless intensity parameter ($q^2 = 1$ corresponds to $I \sim 10^{18}$ W/cm^2). Finally, we state the obvious conclusion that achieving maximum gain requires employing tightly focused laser systems of the highest peak power achievable. Superiority of the axicon fields over those of the linearly polarized ones stems from the fact that the radial axicon field component vanishes on the z axis. In the linearly polarized case, the transverse field components deflect the electron slightly transversely and cause it to lose some of the gained energy back to the field.

Dependence of the electron energy gain on the laser output power is next considered. With multipetawatt laser sys-

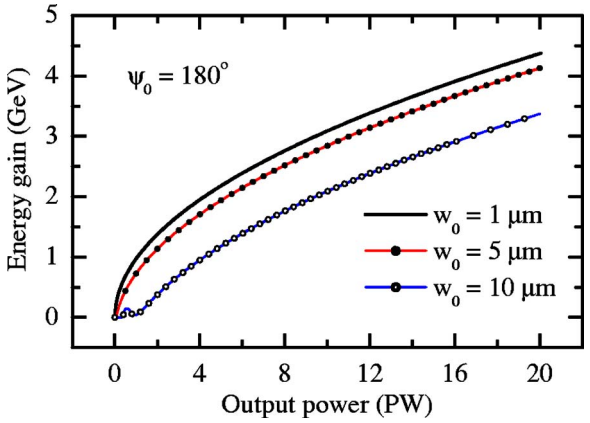

FIG. 3. (Color online) Energy gain of the electron as a function of the laser output power in petawatt (PW). The initial conditions and other parameters are the same as in Fig. 2.

tems in mind, we have calculated variation of the gain as a function of the peak power in petawatt. The most promising scenario, as far as maximum gain is concerned, has been taken: namely, the one corresponding to $\psi_0 \simeq \pi$ and $w_0 = 1$ μm. Our results are shown in Fig. 3. The conclusion that the gain increases monotonically with increasing power is hardly surprising. In fact, earlier order-of-magnitude estimates [11], based on a picture in which interaction of the electron with the laser field is limited to one Rayleigh range, have shown that the gain (in MeV) goes as $C_0\sqrt{P}$, where C_0 is a constant of the order of 20–30 and P is the power in terawatt (TW). Those estimates agree with the results of our accurate calculations shown in Fig. 3.

It has been shown, in earlier careful studies of electron acceleration by linearly polarized Gaussian laser beams [1,5–8], that the most significant energy gain actually takes place over a small region of space centered on the beam focus. In order to investigate this issue in the present scheme, we have calculated variation of the gain with the forward distance of travel of the electron. The results are displayed in Fig. 4(a) for system parameters similar to what has been used in Fig. 2. Note first that the rise in gain is quite sharp from 0 to a maximum (that depends upon the laser power) over a short distance. Evident also in Fig. 4(a) is an increase of the maximum distance of travel with increasing power. With increasing power, the electron gains more energy and travels faster and farther. The energy gained in this way is retained by the electron, as it continues moving forward at a speed close to c.

This description of the electron dynamics may be supported further by looking at the *instantaneous* energy gradient

$$(\text{Energy gradient}) \equiv \frac{d\mathcal{E}}{dz} = -e\left(\frac{\boldsymbol{\beta}\cdot\boldsymbol{E}}{\beta_z}\right), \tag{33}$$

which may be easily arrived at from the second of Eqs. (30). This quantity is shown in Fig. 4(b) for the cases considered in (a). Note that the maxima in the energy gradients are reached at points corresponding to $z < z_r$. Furthermore, $z_r = \pi$ μm for the parameters of Fig. 4. According to Fig. 4, all

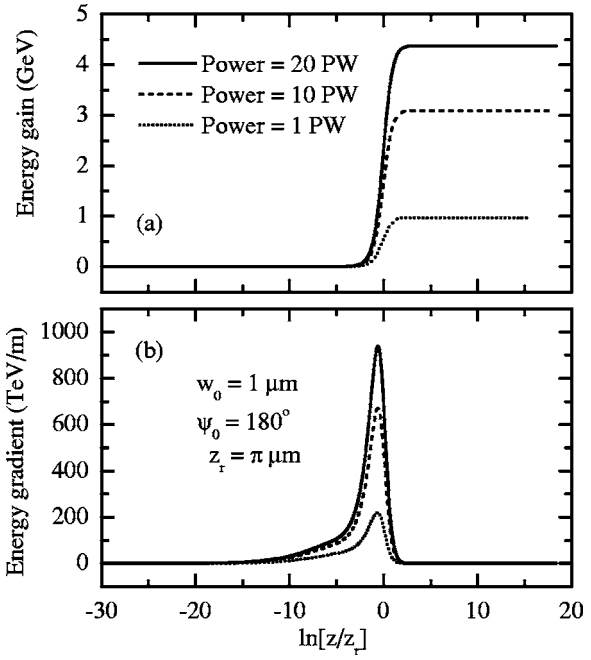

FIG. 4. (a) Energy gain of the electron and (b) its ejection energy gradient, as functions of the logarithm of the forward distance of travel, z, scaled by the Rayleigh length z_r. Scheme parameters not shown are the same as in Fig. 2, and the legends in (a) apply to (b) as well.

acceleration takes place below a value of $\ln[z/z_r]$ roughly less than 4. This corresponds to $z < 55$ $z_r \simeq 170$ μm. Let us adopt a definition for *an average energy gradient* given by the ratio of the total gain to the total distance over which that gain occurs. Then Fig. 4 gives average gradients of about 6, 18, and 26 TeV/m for the three cases considered there. Compared to a maximum energy gradient of 100 MeV/m in conventional microwave-based accelerators, the average gradients in this scheme are roughly 5–6 orders of magnitude higher.

V. CONCLUSIONS AND OUTLOOK

We have shown that lowest-order axicon fields of a petawatt-power laser beam, focused down to a micron-size focal spot, can accelerate electrons from rest to GeV energies. Acceleration results primarily from interaction with the axial electric field component, while the remaining nonzero field components help mainly to confine the electron to a straight-line trajectory along the laser propagation direction. This picture already hints at the possibility of getting a well-collimated accelerated electron beam in a laboratory setup. More practically useful conclusions about electron acceleration may be arrived at from simulations involving an electron bunch, rather than just a single electron.

Our calculations considered only electrons born at rest, maybe from ionization. To employ the scheme as a booster, electron axial injection, perhaps through a hole in the axicon, or injection at an angle to the beam axis, ought to be studied.

Unfortunately, there is much more to laser acceleration than presented by the idealistic calculations of the present

paper. The initial conditions assumed in the scheme are either not plausible or they represent a huge leap into the future at best [33]. A petawatt laser system consumes much more power than the entire electrical generating capacity of the United States [34] and a continuous petawatt beam is not a reality yet. An atom subjected to petawatt power fields gets ionized (and its electrons scatter in all directions) quickly and long before the peak intensity is reached. Thus meeting the initial conditions of the scheme is not presently plausible. These are but a few of the technical issues that make a vacuum laser accelerator scheme quite difficult to realize soon. Finally, we make the remark that the lowest-order fields may not model the tightly focused beam accurately. Proper description of the fields in the regime of tight focusing requires inclusion of terms of higher order in the diffraction angle ε.

ACKNOWLEDGMENT

The author would like to thank K. T. McDonald for suggesting the problem and for critical comments on the practicality of the scheme.

[1] Y. I. Salamin and C. H. Keitel, Phys. Rev. Lett. **88**, 095005 (2002).
[2] L. W. Davis, Phys. Rev. A **19**, 1177 (1979).
[3] J. P. Barton and D. R. Alexander, J. Appl. Phys. **66**, 2800 (1989).
[4] K. T. McDonald, hep.princeton.edu/~mcdonald/accel/gaussian.ps; hep.princeton.edu/~mcdonald/accel/gaussian2.ps
[5] Y. I. Salamin, G. R. Mocken, and C. H. Keitel, Phys. Rev. E **67**, 016501 (2003).
[6] Y. I. Salamin, G. R. Mocken, and C. H. Keitel, Phys. Rev. ST Accel. Beams **5**, 101301 (2002).
[7] Y. I. Salamin and C. H. Keitel, in *Correlation and Polarization in Photonic, Electronic, and Atomic Collisions*, AIP Conf. Proc. No. 697, edited by G. F. Hanne *et al.* (AIP, Melville, NY, 2003), AIP Conf. Proc. **697**, 3 (2003).
[8] Y. I. Salamin and C. H. Keitel, Laser Phys. **13**, 407 (2003).
[9] L. Cicchitelli, H. Hora, and R. Postle, Phys. Rev. A **41**, 3727 (1990).
[10] M. O. Scully and M. S. Zubairy, Phys. Rev. A **44**, 2656 (1991).
[11] E. Esarey, P. Sprangle, and J. Krall, Phys. Rev. E **52**, 5443 (1995).
[12] B. Hafizi, A. Ting, E. Esarey, P. Sprangle, and J. Krall, Phys. Rev. E **55**, 5924 (1997).
[13] B. Hafizi, A. K. Ganguly, A. Ting, C. I. Moore, and P. Sprangle, Phys. Rev. E **60**, 4779 (1999).
[14] J. X. Wang, Y. K. Ho, Q. Kong, L. J. Zhu, L. Feng, W. Scheid, and H. Hora, Phys. Rev. E **58**, 6575 (1998).
[15] J. X. Wang, Y. K. Ho, L. Feng, Q. Kong, P. X. Wang, Z. S. Yuan, and W. Scheid, Phys. Rev. E **60**, 7473 (1999).
[16] L. J. Zhu, Y. K. Ho, J. X. Wang, and L. Feng, J. Phys. B **32**, 939 (1999).
[17] Q. Kong, Y. K. Ho, L. Feng, Q. Kong, P. X. Wang, Z. S. Yuan, and W. Scheid, Phys. Rev. E **61**, 1981 (2000).
[18] Y. Chang and Z. Xu, Appl. Phys. Lett. **74**, 2116 (1999).
[19] P. X. Wang *et al.*, Appl. Phys. Lett. **78**, 2253 (2001).
[20] J. Pang, Y. K. Ho, X. Q. Yuan, N. Cao, Q. Kong, P. X. Wang, L. Shao, E. H. Esarey, and A. M. Sessler, Phys. Rev. E **66**, 066501 (2002).
[21] G. Malka, E. Lefebvre, and J. L. Miquel, Phys. Rev. Lett. **78**, 3314 (1997).
[22] For a review of plasma-based laser accelerators, see R. Bingham, J. T. Mendonca, and P. K. Shukla, Plasma Phys. Controlled Fusion **46**, R1 (2004).
[23] S. P. D. Mangles *et al.*, Nature (London) **431**, 535 (2004).
[24] C. G. R. Geddes *et al.*, Nature (London) **431**, 538 (2004).
[25] J. Faure *et al.*, Nature (London) **431**, 541 (2004).
[26] A. V. Nesterov, V. G. Niziev, and V. P. Yakunin, J. Phys. D **32**, 2871 (1996).
[27] R. Oron *et al.*, Appl. Phys. Lett. **77**, 3322 (2000).
[28] K. T. McDonald, puhep1.princeton.edu/~mcdonald/examples/axicon.pdf
[29] P. Serafim, P. Sprangle, and B. Hafizi, IEEE Trans. Plasma Sci. **28**, 1155 (2000).
[30] J. X. Wang and Y. K. Ho, J. Phys. D **29**, 2796 (1996).
[31] S. Quabis, R. Dorn, M. Eberler, O. Glöckl, and G. Leuchs, Appl. Phys. B: Lasers Opt. **72**, 109 (2001).
[32] R. Dorn, S. Quabis, and G. Leuchs, Phys. Rev. Lett. **91**, 233901 (2003).
[33] K. T. McDonald (private communication).
[34] M. Perry, http://www.llnl.gov/str/Petawatt.html